TABLE II

Effects of FGF-18 on osteoclast formation in the mouse coculture system in the presence and absence of specific inhibitors of cyclooxygenase 2 and RANKL

Data are expressed as means ± S.D. for 8 cultures/group. Representative TRAP staining pictures are shown on the right.

		Number of Osteoclasts / well
Control		18.5±4.8
FGF-18	10^{-12} M	20.5±8.5
	10^{-11}	49.8±7.4
	10^{-10}	99.1±18.2*
	10^{-9}	205.0±50.1*
	10^{-8}	469.1±19.6*
	+NS-398	92.5±16.8#
	+OPG	28.0±3.6#
FGF-2	10^{-8} M	453.3±53.9*
FGF-10	10^{-8} M	20.7±5.0

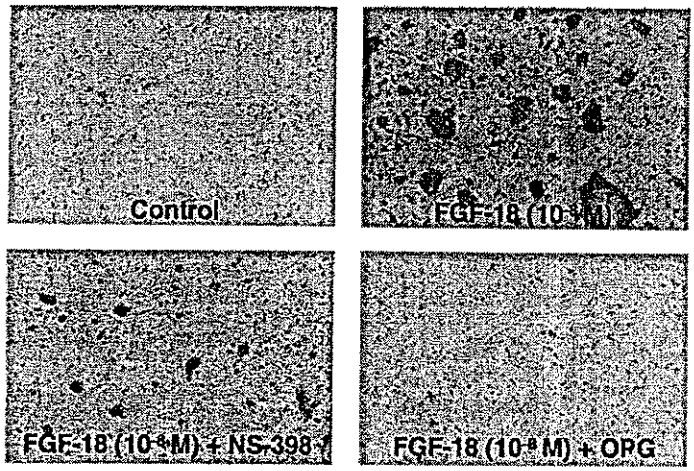

* $p < 0.01$, significant stimulation by FGFs.
\# $p < 0.01$, significant inhibition by NS-398 or OPG (*versus* 10^{-8} M FGF-18 alone).

TABLE III

Effects of FGFs on resorbed pit area, osteoclast number, and the pit area/osteoclast by mouse osteoclasts on a dentine slice

Data are expressed as means ± S.D. for 8 cultures/group.

	Resorbed pit area	Osteoclast no.	Pit area/osteoclast
	$\times 10^3$ μm^2/*dentine*	*cells/dentine*	μm^2/*cell*
Control	356.5 ± 28.9	214.8 ± 25.8	166.3 ± 19.8
FGF-18			
10^{-12} M	477.1 ± 52.2	200.3 ± 21.4	240.5 ± 55.3
10^{-11} M	460.2 ± 52.3	196.5 ± 16.5	234.2 ± 51.8
10^{-10} M	589.3 ± 58.5	218.1 ± 20.9	271.7 ± 55.4
10^{-9} M	1529.5 ± 236.3[a]	227.2 ± 20.7	669.9 ± 173.1[a]
10^{-8} M	2017.3 ± 192.9[a]	251.2 ± 16.5	809.3 ± 194.0[a]
FGF-2 (10^{-8} M)	2104.8 ± 142.9[a]	243.5 ± 18.4	868.4 ± 141.7[a]
FGF-10 (10^{-8} M)	451.3 ± 61.0	207.8 ± 12.9	217.1 ± 53.8

[a] $p < 0.01$, significant stimulation by FGFs.

uronic acid content and extent of sulfation (33). Heparin can activate the mitogenic activity of several FGFs but inhibits that of others (34). Moreover, the effect of heparin on FGF mitogenic activity appears to be cell type-dependent and remains to be elucidated. In this study, the effects of FGF-18 on osteoblasts and chondrocytes did not change when heparin was added to the cultures. It is speculated that endogenous heparan sulfate produced by these cells might be sufficient for FGF-18 to exert mitogenic actions on the cells. Further understanding of the involvement of heparan sulfate in the ligand-receptor interaction might clarify the difference in the mechanism of FGF mitogenic action on several types of cells.

The main signaling pathway of FGF-2 for cell proliferation and differentiation is known to be Ras/MAPK (32, 35–37), although the involvement of other signaling pathways such as protein kinase C, cytoplasmic tyrosine kinase Src, and protein kinase C-independent p70 S6 kinase is also suggested (38, 39). The present study demonstrated that ERK signaling is an important pathway for the mitogenic action of FGF-18 in osteoblasts and chondrocytes. This result shows good correspondence with previous reports suggesting distinct roles for MAPK pathways in regulating the activity of osteoblasts and chondrocytes under several stimulations including FGF-2: the ERK pathway is involved mainly in the control of cell proliferation, whereas the p38 or JNK pathway regulates cell differentiation and function (40–44). In the present study, however, p38 MAPK also mediated FGF-18 mitogenic action in chondrocytes, but not in osteoblasts. Although FGF-18 exhibited inhibitory actions on the differentiation/matrix synthesis of both osteoblasts and chondrocytes, our preliminary investigation using inhibitors of MAPK signaling has thus far failed to identify the signaling mechanism. Signaling pathways other than MAPK pathways as described above might play a role in the inhibition. Additional studies using transfection with signaling molecule-related genes will elucidate the precise mechanism.

Although *Fgf-10*-deficient mice had complete truncation of fore and hind limbs (21), this study showed that FGF-10 affected none of the cultured bone or cartilage cells. Because analyses of the embryos and marker gene expression showed that FGF-10 triggers sequential events for the formation of limbs (20, 21), it is likely to be essential for morphogenesis and organogenesis in embryos, but not for bone or cartilage metabolism in adult tissues.

We have reported that FGF-2 has various physiological, pathological, and pharmacological effects on bone and cartilage metabolism. With regard to the clinical relevance of its action, the pharmacological action of FGF-2 on bone formation has been reported using several *in vivo* models such as fracture healing (10, 11), and study of its clinical application is now underway. On the other hand, endogenous FGF-2 in synovial fluid was positively correlated with the severity of joint destruction in rheumatoid arthritis patients (18). Because FGF-18 showed actions on bone and cartilage cells that bore a close resemblance to those of FGF-2, FGF-18 may compensate for the roles of FGF-2 in a physiological and pathological condition and might be clinically applicable as a potent osteogenic agent.

REFERENCES

1. Ornitz, D. M., and Itoh, N. (2001) *Genome Biol.* 2, 3005.1–3005.12
2. Johnson, D. E., and Williams, L. T. (1993) *Adv. Cancer Res.* 60, 1–41
3. Rousseau, F., Bonaventure, J., Legeal-Mallet, L., Pelet, A., Rozet, J.-M.,

Maroteaux, P., Le, Merrer, M., and Munnich, A. (1994) *Nature* **371**, 252–254
4. Shiang, R., Thompson, L. M., Zhu, Y.-Z., Church, D. M., Fielder, T. J., Bocian, M., Winokur, S. T., and Wasmuth, J. J. (1994) *Cell* **78**, 335–342
5. Webster, M. K., D'Avis, R. Y., Robertson, S. C., and Donoghue, D. J. (1996) *Mol. Cell. Biol.* **8**, 4081–4087
6. Canalis, E., Centrella, M., and McCarthy, T. L. (1988) *J. Clin. Invest.* **81**, 1572–1577
7. Rodan, S. B., Wesolowski, G., Kyonggeun, Y., and Rodan, G. A. (1989) *J. Biol. Chem.* **264**, 19934–19941
8. Hurley, M. M., Abreu, C., Gronowicz, G. A., Kawaguchi, H., and Lorenzo, J. A. (1994) *J. Biol. Chem.* **269**, 9392–9396
9. Aspenberg, P., and Lohmander, L. S. (1989) *Acta Orthop. Scand.* **60**, 473–476
10. Kawaguchi, H., Kurokawa, T., Hanada, K., Hiyama, Y., Tamura, M., Ogata, E., and Matsumoto, T. (1994) *Endocrinology* **135**, 774–781
11. Kawaguchi, H., Nakamura, K., Tabata, Y., Ikada, Y., Aoyama, I., Anzai, J., Nakamura, T., Hiyama, Y., and Tamura, M. (2001) *J. Clin. Endocrinol. Metab.* **86**, 875–880
12. Montero, A., Okada, Y., Tomira, M., Ito, M., Tsurukami, H., Nakamura, T., Doetschman, T., Coffin, J. D., and Hurley, M. M. (2000) *J. Clin. Invest.* **105**, 1085–1093
13. Kawaguchi, H., Pilbeam, C. C., Gronowicz, G., Abreu, C., Fletcher, B. S., Herschman, H. R., Raisz, L. G., and Hurley, M. M. (1995) *J. Clin. Invest.* **96**, 923–930
14. Hurley, M. M., Lee, S. K., Raisz, L. G., Bernecker, P., and Lorenzo, J. (1998) *Bone (NY)* **22**, 309–316
15. Kawaguchi, H., Chikazu, D., Nakamura, K., Kumegawa, M., and Hakeda, Y. (2000) *J. Bone Miner. Res.* **15**, 466–473
16. Chikazu, D., Hakeda, Y., Ogata, N., Nemoto, K., Itabashi, A., Takao, T., Kumegawa, M., Nakamura, K., and Kawaguchi, H. (2000) *J. Biol. Chem.* **275**, 31444–31450
17. Chikazu, D., Katagiri, M., Ogasawara, T., Ogata, N., Shimoaka, T., Takato, T., Nakamura, K., and Kawaguchi, H. (2001) *J. Bone Miner. Res.* **16**, 2074–2081
18. Manabe, N., Oda, H., Nakamura, K., Kuga, Y., Uchida, S., and Kawaguchi, H. (1999) *Rheumatology* **38**, 714–720
19. Yamasaki, M., Miyake, A., Tafashira, S., and Itoh, N. (1996) *J. Biol. Chem.* **271**, 15918–15921
20. Ohuchi, H., Nakagawa, T., Yamamoto, A., Araga, A., Ohata, T., Ishimaru, Y., Yoshioka, H., Nohno, T., Yamasaki, M., Itoh, N., and Noji, S. (1997) *Development* **124**, 2235–2244
21. Sekine, K., Ohuchi, H., Fujiwara, M., Yamasaki, M., Yoshizawa, T., Sato, T., Yagishita, N., Matsui, D., Koga, Y., Itoh, N., and Kato, S. (1999) *Nat. Genet.* **21**, 138–141
22. Ohbayashi, N., Hoshikawa, M., Kimura, S., Yamasaki, M., Fukui, S., and Itoh, N. (1998) *J. Biol. Chem.* **273**, 18161–18164
23. Hu, M. C., Qiu, W. R., Wang, Y. P., Hill, D., Ring, B. D., Scully, S., Bolon, B., DeRose, M., Luethy, R., Simonet, W. S., Arakawa, T., and Danilenko, D. M. (1998) *Mol. Cell. Biol.* **18**, 6063–6074
24. Hu, M. C., Wang, Y. P., and Qui, W. R. (1999) *Oncogene* **18**, 2635–2642
25. Zimmermann, M. (1983) *Pain* **16**, 109–110
26. Beier, F., Lee, R. J., Taylor, A. C., Pestell, R. G., and LuValle, P. (1999) *Proc. Natl. Acad. Sci. U. S. A.* **96**, 1433–1438
27. Schlessinger, J., Lax, I., and Lemmon, M. (1995) *Cell* **83**, 357–360
28. Alessi, D. R., Cuenda, A., Cohen, P., Dudley, D. T., and Saltiel, A. R. (1995) *J. Biol. Chem.* **270**, 27489–27494
29. Lee, J. C., Laydon, J. T., McDonnell, P. C., Gallagher, T. F., Kumar, S., Green, D., McNulty, D., Blumenthal, M. J., Heys, J. R., Landvatter, S. W., Strickler, J. E., McLaughlin, M. M., Siemens, I. R., Fisher, S. M., Livi, G. P., White, J. R., Adams, J. L., and Young, P. R. (1994) *Nature* **372**, 739–746
30. Kameda, T., Miyazawa, K., Mori, Y., Yuasa, T., Shiokawa, M., Nakamura, Y., Mano, H., Hakeda, Y., Kameda, A., and Kumegawa, M. (1996) *Biochem. Biophys. Res. Commun.* **220**, 515–519
31. Xu, J., Liu, Z., and Ornitz, D. M. (2000) *Development* **127**, 1833–1843
32. Bikfalvi, A., Klein, S., Pintucci, G., and Rifkin, D. B. (1997) *Endocr. Rev.* **18**, 26–45
33. Humphries, D. E., and R. L. Stevens (1992) *Adv. Exp. Med. Biol.* **313**, 59–67
34. Turnbull, J. E., Fernig, D. G., Ke, Y., Wilkinson, M. C., and Gallagher, J. T. (1992) *J. Biol. Chem.* **267**, 10337–10341
35. Klint, P., Kanda, S., and Claesson-Welsh, L. (1995) *J. Biol. Chem.* **270**, 23337–23344
36. Kouhara, H., Hadari, Y. R., Spivak-Kroizman, T., Schilling, J., Bar-Sagi, D., Lax, I., and Schlessinger, J. (1997) *Cell* **89**, 693–702
37. Klint, P., Kanda, S., Kloog, Y., and Claesson-Welsh, L. (1999) *Oncogene* **18**, 3354–3364
38. Zhan, X., Plourde, C., Hu, X., Friesel, R., and Maciag, T. (1994) *J. Biol. Chem.* **269**, 20221–20224
39. Kanda, S., Hodgkin, M. N., Woodfield, R. J., Wakelam, M. J., Thomas, G., and Claesson-Welsh, L. (1997) *J. Biol. Chem.* **272**, 23347–23353
40. Suzuki, A., Palmer, G., Bonjour, J. P., and Caverzasio, J. (1999) *Endocrinology* **140**, 3177–3182
41. Chaudhary, L. R., and Avioli, L. V. (1997) *Biochem. Biophys. Res. Commun.* **238**, 134–139
42. Yonekura, A., Osaki, M., Hirota, Y., Tsukazaki, T., Miyazaki, Y., Matsumoto, T., Ohtsuru, A., Namba, H., Shindo, H., and Yamashita, S. (1999) *Endocr. J.* **46**, 545–553
43. Beier, F., Taylor, A. C., and LuValle, P. (1999) *J. Biol. Chem.* **274**, 30273–30279
44. Murakami, S., Kan, M., McKeehan, W. L., and de Crombrugghe, B. (2000) *Proc. Natl. Acad. Sci. U. S. A.* **97**, 1113–1118

ELSEVIER

Gene 298 (2002) 59–68

GENE
AN INTERNATIONAL JOURNAL ON GENES AND GENOMES

www.elsevier.com/locate/gene

Identification and characterization of the human long form of Sox5 (*L-SOX5*) gene

Toshiyuki Ikeda[a], Junwei Zhang[a], Tokuhiro Chano[b], Akihiko Mabuchi[a], Akira Fukuda[c], Hiroshi Kawaguchi[c], Kozo Nakamura[c], Shiro Ikegawa[a,*]

[a]*Laboratory for Bone and Joint Diseases, SNP Research Center, RIKEN (The Institute of Physical and Chemical Research), c/o Institute of Medical Science, University of Tokyo, 4-6-1 Shirokanedai, Minato-ku, Tokyo 108-8639, Japan*
[b]*Departments of Clinical Laboratory Medicine, Shiga University of Medical Science, Otsu, Japan*
[c]*Department of Orthopaedic Surgery, The University of Tokyo, Tokyo, Japan*

Received 22 March 2002; received in revised form 23 July 2002; accepted 26 August 2002
Received by T. Sekiya

Abstract

The Sox (*Sry*-type HMG box) group of transcription factors, which is defined by a high-mobility group (HMG) DNA-binding domain, is categorized into six subfamilies. Sox5 and Sox6 belong to the group D subfamily, which is characterized by conserved N-terminal domains including a leucine-zipper, a coiled-coil domain and a Q-box. Group D Sox genes are expressed as long and short transcripts that exhibit differential expression patterns. In mouse, the long form of *Sox5*, *L-Sox5*, is co-expressed and interacts with *Sox6*; together, these two proteins appear to play a key role in chondrogenesis and myogenesis. In humans, however, only the short form of *Sox5* has previously been identified. To gain insight into Sox5 function, we have identified and characterized human *L-SOX5*. The human *L-SOX5* cDNA encodes a 763-amino-acid protein that is 416 residues longer than the short form and contains all of the characteristic motifs of group D Sox proteins. The predicted L-SOX5 protein shares 97% amino acid identity with its mouse counterpart and 59% identity with human SOX6. The *L-SOX5* gene contains 18 exons and shows similar genomic structure to *SOX6*. We have identified two transcription start sites in *L-SOX5* and multiple alternatively spliced mRNA variants that are distinct from the short form. Unlike the short form, which shows testis-specific expression, *L-SOX5* is expressed in multiple tissues. Like *SOX6*, *L-SOX5* shows strong expression in chondrocytes and striated muscles, indicating a likely role in human cartilage and muscle development.

Keywords: Chondrogenesis; Group D *SOX*; High mobility group; Leucine zipper; Single nucleotide polymorphism

1. Introduction

The Sox (*Sry*-type HMG box) family of transcription factors is related to the testis-determining gene *Sry* and is defined by the presence of a high-mobility group (HMG) DNA-binding domain. Sox proteins interact with DNA through this domain in a sequence-specific manner, binding in the minor groove of DNA and inducing a significant bend (Ferrari et al., 1992; Connor et al., 1994). Therefore, Sox proteins are thought to function as architectural proteins that organize local chromatin structure, assemble other DNA-binding transcription factors and induce correct gene expression (Werner and Burley, 1997; Wolffe, 1994). Sox function is critical to a number of developmental processes, including sex determination (SOX9) (Foster et al., 1994; Wagner et al., 1994), lens development (Sox1, 2 and 3) (Kamachi et al., 1998), T-cell differentiation (Sox4) (van de Wetering et al., 1993), endocardial ridge development (Sox4) (Schilham et al., 1996), developing cardiac and skeletal muscle systems (Sox6) (Hagiwara et al., 2000) and neural crest cell differentiation (Sox10) (Southard-Smith et al., 1998).

Sox proteins are categorized into six subfamilies based on sequence homology within the HMG box and other domains (Pevny and Lovell-Badge, 1997). The group D subfamily consists of Sox5, Sox6 and Sox13. Although many Sox proteins are encoded by a single exon, group D Sox genes contain multiple exons with conserved genomic structure (Wunderle et al., 1996; Argentaro et al., 2000). They also

Abbreviations: bp, base pair(s); DIG, digoxigenin; cDNA, complementary DNA; HMG, high-mobility group; kb, kilobase(s); *L-SOX5*, long form of *SOX5*; nt, nucleotide(s); RACE, rapid amplification of cDNA ends; RT–PCR, reverse transcription–polymerase chain reaction; *Sox*, *Sry*-type HMG box gene; *Sry*, sex-determining region Y gene; UTR, untranslated region

* Corresponding author. Tel./fax: +81-3-5449-5393.
E-mail address: sikegawa@ims.u-tokyo.ac.jp (S. Ikegawa).

0378-1119/02/$ - see front matter
PII: S0378-1119(02)00927-7

share conserved N-terminal domains, including a leucine zipper, coiled-coil domains and a glutamine-rich region (Q-box), as well as the highly conserved HMG domain (Kido et al., 1998), which are considered critical to their function.

Group D Sox genes are known to express two types of alternatively spliced transcripts, short and long forms (Hiraoka et al., 1998; Argentaro et al., 2000). The short form is a component of the long form, and it lacks the characteristic N-terminal domains. The two forms exhibit different expression patterns: in mouse, the short forms of *Sox5* and *Sox6* are predominantly expressed in testis (Connor et al., 1995; Denny et al., 1992). In contrast, the long form of *Sox6* is expressed in multiple tissues, especially in skeletal muscle, and the long form of *Sox5* (*L-Sox5*) is primarily expressed in cartilage (Lefebvre et al., 1998). Co-expressed with *Sox9* during chondrogenesis, *L-Sox5* and *Sox6* heterodimerize via their coiled-coil domains and activate the type II collagen gene (*Col2A1*), which encodes a major matrix component protein in cartilage (Lefebvre et al., 1998).

In humans, only the short form of the *SOX5* gene has previously been identified (Wunderle et al., 1996). This short form shares high homology with mouse *Sox5*. Human SOX6, which is predicted to interact with the long form of SOX5, has recently been identified (Cohen-Barak et al., 2001). These facts strongly support the existence of a long form of human SOX5 (L-SOX5). Identification of the human *L-SOX5* gene will be an important first step toward determining the precise role of the group D SOX genes in human chondrogenesis and other developmental pathways.

Here we report the isolation and characterization of the human *L-SOX5* gene. *L-SOX5* contains all cardinal motifs common to group D SOX proteins. Like its mouse counterpart, *L-SOX5* has multiple transcriptional start sites and multiple alternative splicing variants, but it shows a unique expression pattern in human tissues.

2. Materials and methods

2.1. 5′- and 3′-RACE

To extend the *SOX5* sequence in the 5′- and 3′-directions, we performed rapid amplification of cDNA ends (RACE). Because mouse *L-Sox5* is expressed in both liver and cultured chondrocytes, and human *SOX5* is expressed in testis, we used Marathon-Ready human liver and testis cDNAs (Clontech, Palo Alto, CA) and a custom-made cultured human chondrocyte cDNA template prepared using the Marathon cDNA Amplification Kit (Clontech) as templates, according to the manufacturer's instructions.

The 5′-RACE was performed using two sets of first and nested primers. The first set of gene-specific primers, 5′-CCTTGAACCTGGATCTGTTGCTGGA-3′ (first) and 5′-CTGCTTGGCCAGCTCCATTTGCT-3′ (nested), was designed based on published human *SOX5* cDNA sequence (GenBank accession no. S83308). Products from the first amplification were cloned into the TOPO-pCR2.1 vector (Invitrogen, Carlsbad, CA) and sequenced. A second PCR reaction was performed using the primers 5′-AAAGGCTGGGAGCCCGTCACTCT-3′ (first) and 5′-CTTCCCCATACGGAGAGGCTGGTC-3′ (nested), which were designed based on cDNA sequence obtained from the first amplification. The resulting PCR products were subcloned and sequenced.

The 3′-RACE was carried out in a similar fashion. The first set of gene-specific primers consisted of 5′-GGTTCATCCTTACCAGTGGCCAAGC-3′ (first) and 5′-GACCTCAGCCTCAAAAGGCTTGGAA-3′ (nested). The second set consisted of 5′-TGGGGATGAAATCCCA-CATCCT-3′ (first) and 5′-TCTGGGGATGAAATCCCA-CATCC-3′ (nested).

2.2. Cell lines and cultures

The human chondrosarcoma-derived cell line, CS-OKB was as previously described (Chano et al., 1998). OUMS-27 cells that also derived from human chondrosarcoma (Kunisada et al., 1998) were purchased from IFO Animal Cell Bank (Osaka, Japan). The human chondrocyte cell line was purchased from Cell Applications Inc. (San Diego, CA). The HepG2 (RCB1648) and HuH-7 (RCB1366) cell lines were provided by Riken Cell Bank (Tsukuba, Japan). CS-OKB cells were maintained in RPMI1640 medium (Sigma, St. Louis, MO) with 10% fetal bovine serum (FBS) (Gibco BRL Inc., Washington, DC), OUMS-27 and HuH-7 cells were maintained in Dulbecco's modified Eagle's medium-high glucose (Sigma) with 10% FBS. HepG2 cells were maintained in minimal essential medium (Sigma) with 0.1 mM non-essential amino acids and 10% FBS. All cell culture media were supplemented with penicillin (50 units/ml) and streptomycin (50 mg/ml). Human chondrocytes were maintained in special medium according to the manufacturer's instructions

2.3. Preparation of genomic DNA

Genomic DNA from 16 Japanese individuals was extracted from peripheral blood leukocytes using a Genomix kit (Talent, Trieste, Italy). These individuals were participants in the Genetic Study Program of Bone and Joint Diseases at Tokyo University and its related institutes. Written informed consent was obtained from each participant.

2.4. Preparation of poly(A)$^+$ RNA

Total RNA was extracted from cell lines and cultured human chondrocytes using ISOGEN (Nippon Gene, Tokyo, Japan), and poly(A)$^+$ RNA was prepared using the PolyATtract mRNA Isolation System (Promega, Madison, WI), according to the manufacturer's protocol.

2.5. PCR amplification of L-SOX5 cDNA

Through 5′-RACE analysis, we identified two major long SOX5 transcripts with different transcriptional start sites and 5′-UTR sequences. To confirm the existence of these transcripts, we amplified the entire coding sequence using two primer sets complementary to the 5′- and 3′-UTR regions of the L-SOX5 gene. The first primer set consisted of 5′-AAAGGGAAATTGTGCTTTTCCAG-3′ and 5′-GGGCTTCTTTAAGTCCTAAGGTCA-3′, and the second primer set was 5′-GCTGAACAGAGAATTCTGGCACT-3′ and 5′-TATCAGTTGGCTTGTCCTGCAAT-3′. The cDNA sequence of the 3′-UTR was also amplified using the primer set 5′-ACCCAAAAGCAAGGATGAAGTG-3′ and 5′-GGGGGTGAGATAGGAAAATGATG-3′ (corresponding to nt 1154–4259 in Fig. 1). This inter-exon PCR primer set was designed to eliminate contamination by genomic DNA. cDNAs from several tissues, including those used for RACE analyses, were used as templates in these PCR amplifications. The obtained PCR products were subcloned and sequenced to identify alternative splicing variants.

2.6. Analysis of alternative splicing variants

To identify expression pattern of exon 5-alternative splicing variants in various tissues, RT–PCR analysis was performed with a primer set of 5′-GGAGTTCC-CAGGGCTGTACT-3′ and 5′-AGGTAGCCATGGTGA-CAAGC-3′ which spanned exons 5 and 6. Total RNAs (500 ng) from the Human Total RNA-Master Panel II (Clontech) were reverse-transcribed using MultiScribe Reverse Transcriptase (ABI, Foster City, CA, USA) and random hexamers in 50 μl reaction volume according to the manufacturer's protocol, and 1 μl of each RT reaction was used as a template for the second-step PCR. PCR fragments were analysed by 4% agarose gel electrophoresis.

2.7. SYBR Green real-time RT–PCR

To quantify expression of the two transcripts (designated A and B) that had different transcription start sites, a two-step SYBR Green real-time RT–PCR (Qiagen, Hilden, Germany) was performed. Total RNAs were reverse-transcribed as described in the previous section, and 1 μl of each RT reaction (10 ng per well, respectively) was used as the template for SYBR Green PCR. SYBR Green PCR amplification and real-time fluorescence detection was performed by a 7700 sequence detection system (ABI) using two unique sense primers, 5′-GACGATCATAGGTGGCTG-CT-3′ (for the A transcript) and 5′-TGATGACAT-GATTCCTGTTTGA-3′ (for the B transcript), and a common anti-sense primer (5′-TGGCTACCTCTC-CATCTGCT-3′). Both primer sets were designed to create approximately 140 bp amplicons. The plasmid DNAs that contained 5′-UTR sequences of the A or B transcript were linearized by *Xho*I digestion, respectively, and used as standard templates. QuantiTect SYBR Green PCR Master Mix (Qiagen) was used for the reaction according to the manufacturer's protocol. Copy numbers of the A and B transcripts in each total RNAs were calculated using standard curve methods, and the ratios of the both transcripts were determined. All reactions were run in quadruplicate.

2.8. Northern blotting

Northern blot analysis was performed using a human multiple-tissue Northern blot membrane (Clontech), as well as poly(A)$^+$ RNA extracted from several liver and cartilage cell lines and cultured human chondrocytes. Poly(A)$^+$ RNA was separated on a 2% formaldehyde gel along with digoxigenin (DIG) labeled RNA molecular weight marker I (Roche, Manheim, Germany), and blotted to nylon membranes by overnight capillary transfer. A 498 bp fragment of *L-SOX5*-specific cDNA (nt 546–1038) was PCR amplified and cloned into the TOPO pCR2.1 vector (Invitrogen). The *L-SOX5* clone was linearized by *HindIII* digestion, and a DIG-labeled *L-SOX5* antisense-RNA probe was prepared by in vitro transcription using a DIG RNA labeling kit (Roche). After overnight hybridization, the RNA probe was detected by chemiluminescence using anti-DIG AP antibody (Roche) and CDP-Star substrate (Tropix Inc., Bedford, MA) (Holtke et al., 1995).

2.9. Analysis of genomic organization and screening of sequence variants

Exon–intron boundaries of *L-SOX5* were identified for comparison of the *L-SOX5* cDNA sequence with genomic sequences in public databases (accession nos. AC087319, AC022359, AC087244, AC034120, AC069208, AC087312). Genomic regions not identified through this approach were cloned using a Genome-Walker kit (Clontech) (Siebert et al., 1995), or by direct PCR amplification of unknown introns. Intron 8 was amplified using the primer set 5′-AGCGTCAGCAAATGGAGCTG-3′ and 5′-TGGAG-CAAATTGATTTTGTGTTG-3′. Genome-walker analysis was performed using three gene-specific primer sets: S5G31 (for the intron 7 acceptor site), 5′-TGCTTGGCCAGCTC-CATTTGCT-3′ (first) and 5′-TACCCATGAGTTGCCTTT-CTTTCTCA-3′ (nested); S5G34 (for the intron 6 acceptor site), 5′-TGCAAGAAGCTTGTCTTTCCAGTCC-3′ (first) and 5′-TGCAAGAAGCTTGTCTTTCCAGTCC-3′ (nested); S5G35 (for the intron 7 donor site), 5′-CTCTCAAAG-GACTGGAAAGACAAGC-3′ (first) and 5′-AGACAAGC-TTCTTGCAATGGGATCG-3′ (nested).

Finally, based on sequences obtained through database searches or Genome-walker analysis, all exons and their flanking regions were PCR amplified from genomic DNA of 16 individuals. Direct sequencing was performed on both strands to confirm the genomic sequence of *L-SOX5* and identify variations within the *L-SOX5* gene.

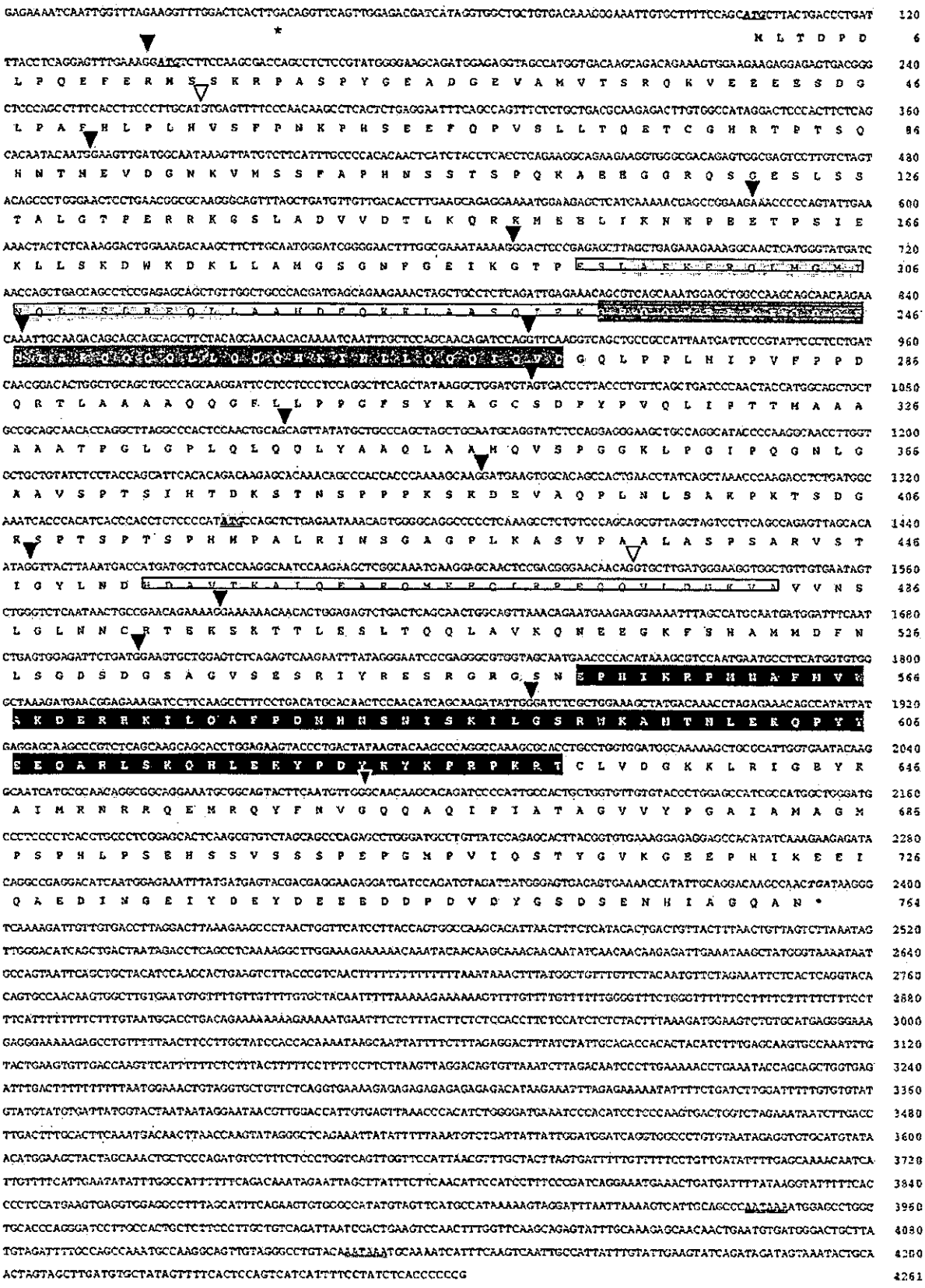

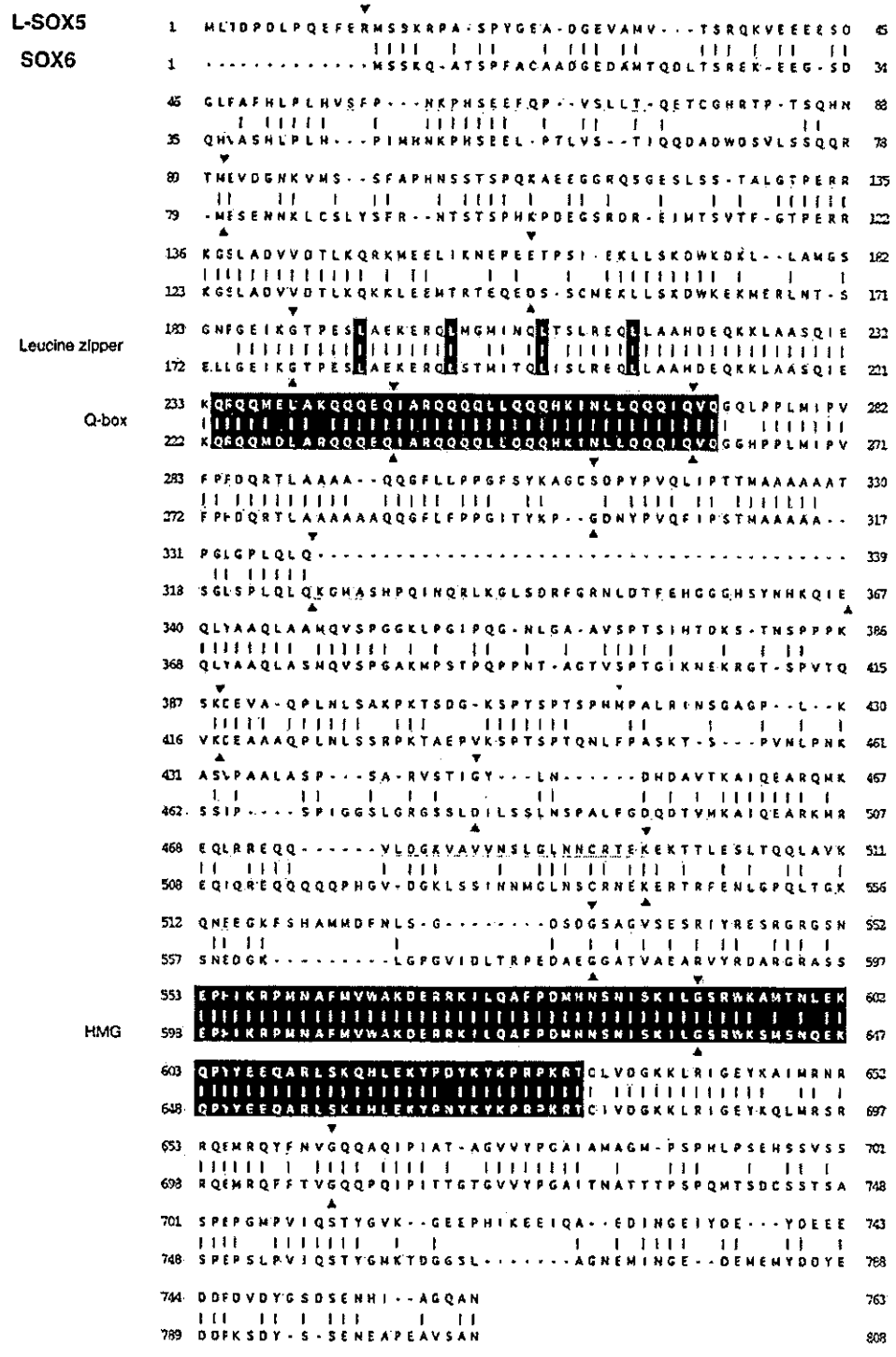

Fig. 2. Alignment of human L-SOX5 and SOX6 amino acid sequences. Numbers refer to amino acid positions in the proteins. Sequences were aligned using the DNAsis version 3.7 program (Hitachi software engineering, Tokyo, Japan). Identical amino acids are linked by vertical lines. The exon/exon boundaries are marked with arrowheads. The *Sry*-related HMG box is indicated by white letters in black boxes. The Q-box is indicated by white letters in gray boxes. The individual leucines of the leucine-zipper motif are also shown by white letters in black boxes. The alternatively spliced sequences are underlined.

transcripts (Fig. 3a). One transcript (A transcript) contained an initiating methionine in exon 1a; another (B transcript) had four non-coding exons, and the initiating methionine was located in exon 5, which was the first exon common to both transcripts. This translation start site in exon 5 is in a comparable position to that of *SOX6* (Cohen-Barak et al.,

Table 1
Human L-SOX5 exon–intron boundaries[a]

Exon no.	Exon size (bp)	Splice acceptor	Splice donor
1a	140	–	AGTTTGAAAG **gtgagtacag**
1b	115	–	ACCGGGTAAG **gtgcgtgaat**
2	82	**tctttttctag** GCTTTTTAAA	AATGTGGCAG **gtgggtctct**
3	77	**tatatcccag** GTGCTGTGCT	ACCTACTGGG **gtatgtacaa**
4	97	**atttttccag** CTTTCCTCTT	TAGGAAAAAG **gtatattcat**
5a	232	**ttccttccag** GATGTCTTCC	CAATACAATG **gtaggtttct**
5b	127	= 5a	TCCCTTGCAT **gtgagttttc**
6	211	**tctctttcag** GAAGTTGATG	GAGCCGGAAG **gtaaaggctg**
7	87	**ctttacttag** AAACCCCCAG	GAAATAAAAG **gtaatatggt**
8	173	**tgatttgtag** GGACTCCCGA	ACAAGAACAA **gtgagtaaga**
9	69	**ttcttcacag** ATTGCAAGAC	ACAGATCCAG **gtcagaaatc**
10	121	**cgttcagcag** GTTCAAGGTC	GCTGGATGTA **gtaagtactg**
11	86	**tcttacttag** GTGACCCTTA	CCAACTGCAG **gtaagtcagg**
12	147	**tcttctgtag** CAGTTATATG	CAAAAGCAAG **gtacccttttt**
13	178	**atcattgcag** GATGAAGTGG	AGCACAATAG **gtaagttctg**
14a	146	**tcatgttcag** GTTACTTAAA	AACAGAAAAG **gtcagttcat**
14b	83	= 14a	GGAACAACAG **gtgcttgatg**
15	109	**ttttttaaag** GAAAAAACAA	GATTCTGATG **gtttgtgaaa**
16	174	**ctgttttcag** GAAGTGCTGG	AAGATATTGG **gtaagaaaac**
17	217	**ttcttcatag** GATCTCGCTG	TCAATGTTGG **gtatgtacct**
18	2171	**ttcttgacag** GCAACAA_CA	–

[a] Ten bases on either side of the exon–intron boundary are shown for each junction. Exonic sequence is indicated in capital letters, with the splice acceptor and splice donor sequences shown in boldface.

3. Results

3.1. Identification of cDNAs encoding human L-SOX5

Through 5′-RACE analysis, we identified two distinct *L-SOX5* transcripts. The longest cDNA sequence obtained by RACE analysis, along with its deduced amino-acid sequence, is shown in Fig. 1 (DDBJ accession no. AB081588). The cDNA sequence contains an open reading-frame that encodes a 763-amino-acid protein, which exceeds the length of the *SOX5* short form (GDB 5584271) by up to 416 amino acids. The translation start site for the short form of *SOX5* is located at codon 417 in *L-SOX5*. An in-frame termination codon is present 64 nucleotides upstream of the putative initiating methionine. Putative poly(A) signals (AATAAA) are located at nt 3943–3948 and 4128–4133.

Human L-SOX5 protein contains several functionally critical domains common to other group D Sox proteins, including the leucine zipper motif, the Q-box (glutamine rich region) (Kido et al., 1998), two coiled-coil domains and the HMG domain. The human and mouse L-SOX5 protein sequences share 97% amino acid identity, and L-SOX5 and human SOX6 proteins share 59% identity (Cohen-Barak et al., 2001). L-SOX5 and SOX6 were 100% identical within the HMG domain and 93% identical within the functionally critical N-terminal region that includes the leucine zipper motif, the coiled-coil domain and the Q-box (Fig. 2).

3.2. Genomic structure of human L-SOX5

Exon–intron boundaries of *L-SOX5* and their flanking sequences are shown in Fig. 1 and Table 1. Human *SOX5* has previously been mapped to chromosome 12p12, and all genomic sequences obtained from comparison of the *L-SOX5* cDNA sequence with public database entries mapped within this region. Sequences flanking exons 7 and 8 could not be obtained from public databases and were instead determined experimentally (AB081590 AB081591). Sequences of all exons along with their flanking intronic sequences were confirmed by direct sequencing of PCR products from genomic DNA of 16 individuals. All exon–intron boundaries were conserved between *L-SOX5* and *SOX6* (Cohen-Barak et al., 2001).

3.3. Alternative splicing of human L-SOX5

We identified at least two major transcription start sites and two different translation initiation codons in the *L-SOX5*

Fig. 1. Nucleotide sequence of the human *L-SOX5* cDNA and its deduced amino acid sequence. Nucleotides and amino acids are numbered on the right. In-frame stop codons are indicated with an asterisk. The two different translation start sites (ATG) are shown in italic bold letters with underlines. The translational start site for the short form of *SOX5* is also shown in italic bold letters and is double-underlined. The Sry-related HMG box is indicated by white letters in black boxes. The Q-box is indicated by white letters in a gray box. The two coiled-coil domains are box-shaded. The leucine zipper motif is gray-shaded. Polyadenylation signals (AATAAA) are double-underlined. Exon/exon boundaries are marked with arrowheads, and the exon–intron boundaries of the alternatively spliced exons are marked with open arrowheads.

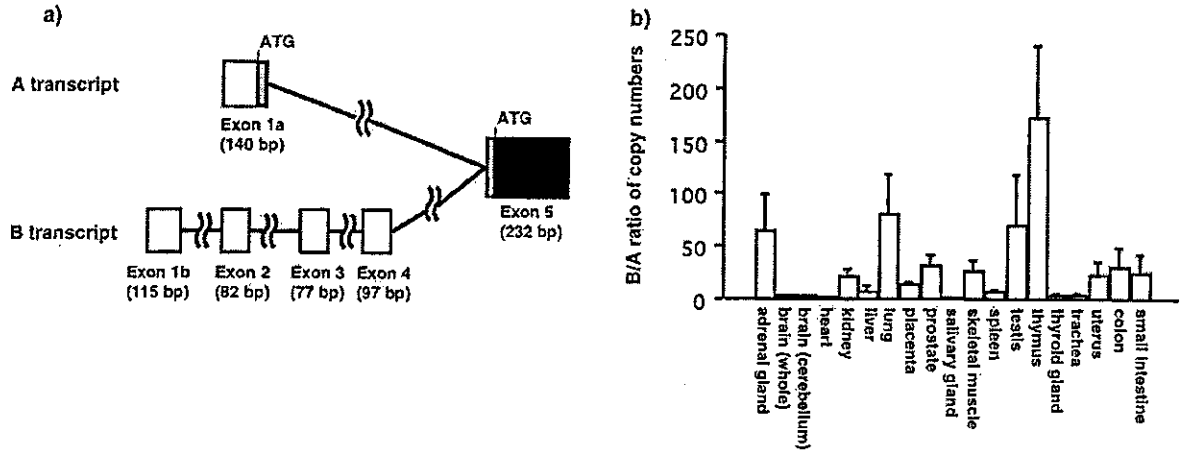

Fig. 3. Variation in the transcription start site of *L-SOX5*. (a) A scheme for the exon structure of the two transcription start-site variants of *L-SOX5*. One transcript (A transcript) starts from exon 1a that contains an in-frame upstream stop codon and the putative translation start site (ATG); another transcript (B transcript) which starts from exon 1b has four non-coding exons that contain no ATG codon after an in-frame stop codon. The first common exon between the two transcripts is exon 5, and the B transcript has a putative translation start site in this exon. (b) Relative amount of the two transcripts. The A and B transcripts were quantified by a real-time RT–PCR analysis and the relative ratio (B/A) was determined. The B transcript is more abundant than the A transcript in all tissues examined.

2001). The 5′-UTR sequence of this transcript was also registered (AB081589). Real-time RT–PCR analysis revealed that both transcripts were expressed in various tissues, and the B transcript was more abundant than the A transcript in all tissues. The ratio of the transcripts (B/A) was different among tissues (Fig. 3b).

L-SOX5 also contained an alternative splicing site in exon 5. Comparison of two published mouse cDNA sequences (Hiraoka et al., 1998; Lefebvre et al., 1998) revealed an alternative splicing of the mouse L-Sox5 at the corresponding position in the corresponding exon. In human, this exon-5 alternative splicing was observed in various tissues, although no tissue-specific expression pattern was determined (Fig. 4). This splicing event did not involve the highly conserved region critical to SOX5 function. The alternative splicing was not detected by Northern analysis, probably because of the small size difference between the splicing variants.

5′-RACE analysis also confirmed the existence of the short form of *SOX5*, which corresponds to exons 13-18 of *L-SOX5*, in a testis cDNA library. The short form contained a non-coding exon located between exons 12 and 13 of the long form and was not present in chondrocyte or liver cDNA samples.

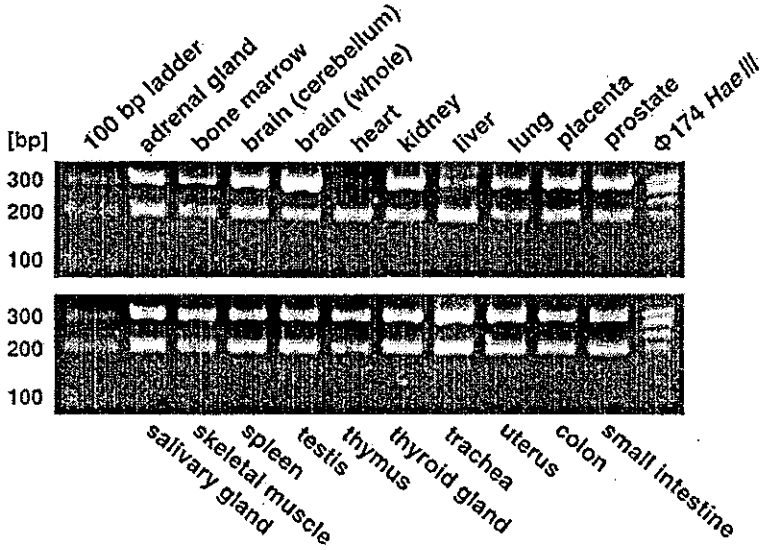

Fig. 4. Tissue distribution of the exon 5-alternative splicing variants. RT–PCR analysis using a set of primers encompassing alternatively-spliced site produces 310 and 204 bp products, both of which are expressed in multiple tissues. In heart and liver, the smaller product is predominant.

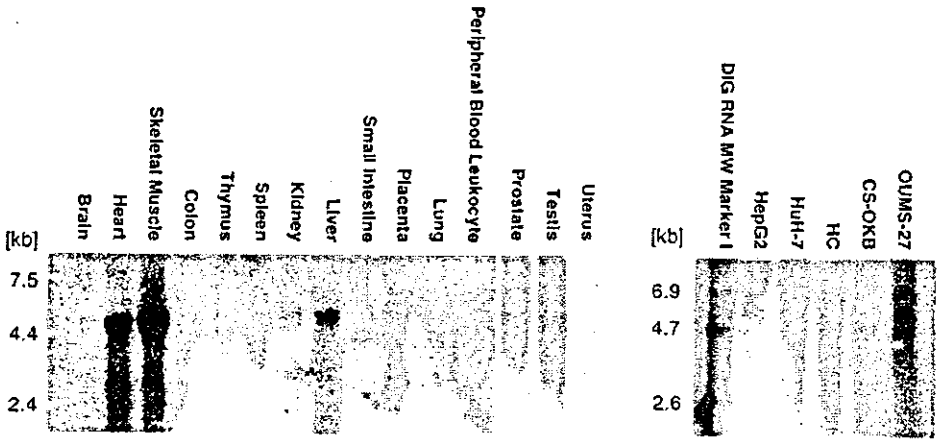

Fig. 5. Northern analyses of *L-SOX5* in human multiple tissues and human cell lines. The filters were hybridized with DIG-labeled human *L-SOX5*-specific cDNA fragments (nt 546–1038). Each lane of the cell line blot contains 500 ng of poly(A)$^+$ RNA. *L-SOX5* is expressed in various tissues, most predominantly in heart, skeletal muscle and liver. It is also expressed in cultured human chondrocytes (HC) and the two human chondrosarcoma-derived cell lines, CS-OKB and OUMS-27.

3.4. Expression of human L-SOX5

Expression of *L-SOX5* mRNA in human tissues and cell lines is shown in Fig. 5. An approximately 5 kb transcript was expressed in various tissues, most predominantly in heart, skeletal muscle and liver. This transcript was shorter than that of mouse *L-Sox5* (7.4 kb) and comparable to the transcripts shown in Fig. 1. *L-SOX5* was also expressed in cultured chondrocytes and the two human chondrosarcoma-derived cell lines, CS-OKB and OUMS-27, which showed cartilage phenotypes (Chano et al., 1998; Kunisada et al., 1998).

3.5. Sequence variations within human L-SOX5

We scanned all exons and ~100 bp of each flanking intronic region to identify polymorphic loci in the human *L-SOX5* gene. Table 2 shows loci for which at least two minor alleles were detected in the 16 individuals analysed; these loci and are thus expected to be common in general population. We identified five variant loci in *L-SOX5*; three were located in the promoter region, and two occurred in introns. Our screen did not detect any variant that resulted in an amino acid substitution. One silent coding SNP (ca. 630C > A) was detected, but only one minor allele of this SNP was detected among 32 chromosomes.

Table 2
Single nucleotide polymorphisms in human L-SOX5 gene

Position	Nucleotide change	Allelic frequency[a] (No. of chromosomes)
Upstream of exon 1a	−943G > A	8/32
Upstream of exon 1a	−842G > A	7/32
Upstream of exon 1a	−713C > G	7/32
Intron 6	IVS6 + 29G > A	5/32
Intron 16	IVS16 + 29A > G	13/32

[a] Allelic frequency of the minor alleles is shown.

4. Discussion

We have identified the human *L-SOX5* cDNA. The predicted human L-SOX5 protein, which is more than twice as large as the short form, contains motifs that are characteristic of group D Sox proteins but absent from the short form. These motifs are highly conserved between L-SOX5 and SOX6, and between human and mouse L-Sox5. This intra-familial and inter-species conservation highlights the importance of these motifs in the function of group D Sox genes. In mouse, L-Sox5 and Sox6 proteins form homo- or heterodimers through their coiled-coil domains and recognize pairs of HMG-binding sites (Lefebvre et al., 1998). This interaction between L-SOX5 and SOX6 is thought to be common between human and mouse and essential to SOX function.

The exact function of *L-SOX5* remains elusive. In mouse, *L-Sox5* is primarily expressed in cartilage, and its expression is associated with the chondrocyte phenotype (Lefebvre et al., 1998). Sox5-deficient mice show a chondrodysplasia-like phenotype (Smits et al., 2001). During the pre-developmental phase of cartilage, *L-Sox5* and *Sox6* are co-expressed with *Sox9*, and they trans-activate *Col2A1* in the presence of *Sox9* (Lefebvre et al., 1998). *Sox9* is a critical transcription factor in cartilage development (Bell et al., 1997; Lefebvre et al., 1997); in humans, *SOX9* mutation causes campomelic dysplasia, a skeletal dysplasia characterized by severe chondrodysplasia and sex-reversal (Foster et al., 1994; Wagner et al., 1994). In this study, we have observed expression of human *L-SOX5*

in chondrocyte and chondrocytic cell lines. Together, these findings suggest an important role for L-SOX5, in concert with SOX6 and SOX9, in human cartilage development.

L-Sox5 also exhibits species-specific differences in expression patterns. In situ hybridization of mouse embryos shows *L-Sox5* expression primarily in cartilage, co-localized with *Col2A1* and *Sox9* transcripts. Northern analysis shows strong expression of *L-Sox5* in primary chondrocytes, chondrogenic cell lines and brain, weak expression in fetal liver, and no expression in skeletal muscle and heart (Lefebvre et al., 1998). We have observed human *L-SOX5* expression in chondrocytes and chondrocytic cell lines; however, it is also strongly expressed in skeletal muscle and heart, similar to *SOX6*. The different expression pattern suggests that in human *L-SOX5* performs multiple functions in various tissues other than *COL2A1* trans-activation. Therefore, regulatory mechanism of the human and mouse L-Sox5 gene may be different. Further analysis of the promoter sequences in human and mouse would address this interesting issue. Currently, we could not find any information about mouse L-Sox5 promoter sequences.

Strong expression of *L-SOX5* and *SOX6* in skeletal muscle and heart suggests potential roles in human myogenesis. Interestingly, mice homozygous for a Sox6 mutation (p^{100H}) show abnormal ultrastructure of skeletal and cardiac muscle. The p^{100H} mutant develops a widespread myopathy that affects skeletal and cardiac myocytes (Hagiwara et al., 2000), providing strong evidence for the importance of *Sox6* in striated muscle development. Because *L-SOX5* is co-expressed and intimately interacts with *SOX6*, it may also play a similar role in human muscle development.

The wide range of expression of the long form of *SOX5* contrasts with the testis-specific expression of the short form (Wunderle et al., 1996) implying very different functions for the two forms. The short form lacks N-terminal motifs critical to function as a transcription factor and association with *SOX6*. Expression analysis in the adult mouse revealed that Sox5 proteins were restricted to the nuclei of haploid round spermatids within the testis (Connor et al., 1994). Therefore, the short form of *SOX5* is likely to play a limited and specialized role in testis development.

The human *L-SOX5* gene shows complex splicing patterns, containing at least two major transcription start sites that are distinct from that for the short form. Although the B transcript lacks the N-terminal 13 amino acids of the A transcript, the protein product of this transcript is likely to be as functional as the A transcript because of its predominance in multiple tissues and homology to SOX6 protein. *L-SOX5* also has an alternative splicing site in exon 5. Because no tissue-specific expression pattern was observed, and because the variable region did not contain the highly conserved motifs, this splice variant is unlikely to have functional significance. Minor functional variances conferred by alternative splicing may be needed for some specific developmental process, however.

In conclusion, we have identified the human *L-SOX5* cDNA sequence, determined its genomic organization and examined its expression. The expression pattern of *L-SOX5* suggests potentially different functions from its mouse counterpart and the short, alternatively spliced form. Human *L-SOX5* is likely to play important roles in chondrogenesis and development of striated muscles. Further analysis of the L-SOX5 gene should reveal novel functional information about musculoskeletal development and its related diseases.

Acknowledgements

We thank Drs. Masayoshi Namba and Hidetoshi Okabe for help in performing study of cell line cultures, and Mss. Aya Narita and Tomoko Kusadokoro for excellent technical assistance.

References

Argentaro, A., Olsson, J., Critcher, R., McDowall, S.G., Harley, V.R., 2000. Genomic characterisation and fine mapping of the human SOX13 gene. Gene 250, 181–189.

Bell, D.M., Leung, K.K., Wheatley, S.C., Ng, L.J., Zhou, S., Ling, K.W., Sham, M.H., Koopman, P., Tam, P.P., Cheah, K.S., 1997. SOX9 directly regulates the type-II collagen gene. Nat. Genet. 16, 174–178.

Chano, T., Okabe, H., Saeki, Y., Ishizawa, M., Matsumoto, K., Hukuda, S., 1998. Characterization of a newly established human chondrosarcoma cell line, CS-OKB. Virchows Arch. 432, 529–534.

Cohen-Barak, O., Hagiwara, N., Arlt, M.F., Horton, J.P., Brilliant, M.H., 2001. Cloning, characterization and chromosome mapping of the human SOX6 gene. Gene 265, 157–164.

Connor, F., Cary, P.D., Read, C.M., Preston, N.S., Driscoll, P.C., Denny, P., Crane-Robinson, C., Ashworth, A., 1994. DNA binding and bending properties of the post-meiotically expressed Sry-related protein Sox-5. Nucleic Acids Res. 22, 3339–3346.

Connor, F., Wright, E., Denny, P., Koopman, P., Ashworth, A., 1995. The Sry-related HMG box-containing gene Sox6 is expressed in the adult testis and developing nervous system of the mouse. Nucleic Acids Res. 23, 3365–3372.

Denny, P., Swift, S., Connor, F., Ashworth, A., 1992. An SRY-related gene expressed during spermatogenesis in the mouse encodes a sequence-specific DNA-binding protein. EMBO J. 11, 3705–3712.

Ferrari, S., Harley, V.R., Pontiggia, A., Goodfellow, P.N., Lovell-Badge, R., Bianchi, M.E., 1992. SRY, like HMG1, recognizes sharp angles in DNA. EMBO J. 11, 4497–4506.

Foster, J.W., Dominguez-Steglich, M.A., Guioli, S., Kowk, G., Weller, P.A., Stevanovic, M., Weissenbach, J., Mansour, S., Young, I.D., Goodfellow, P.N., Brook, J.D., Schafer, A.J., 1994. Campomelic dysplasia and autosomal sex reversal caused by mutations in an SRY-related gene. Nature 372, 525–530.

Hagiwara, N., Klewer, S.E., Samson, R.A., Erickson, D.T., Lyon, M.F., Brilliant, M.H., 2000. Sox6 is a candidate gene for p100H myopathy, heart block, and sudden neonatal death. Proc. Natl. Acad. Sci. USA 97, 4180–4185.

Hiraoka, Y., Ogawa, M., Sakai, Y., Kido, S., Aiso, S., 1998. The mouse Sox5 gene encodes a protein containing the leucine zipper and the Q box. Biochim. Biophys. Acta 1399, 40–46.

Holtke, H.J., Ankenbauer, W., Muhlegger, K., Rein, R., Sagner, G., Seibl, R., Walter, T., 1995. The digoxigenin (DIG) system for non-radioactive labelling and detection of nucleic acids – an overview. Cell Mol. Biol. (Noisy-le-grand) 41, 883–905.

Kamachi, Y., Uchikawa, M., Collignon, J., Lovell-Badge, R., Kondoh, H., 1998. Involvement of Sox1, 2 and 3 in the early and subsequent molecular events of lens induction. Development 125, 2521–2532.

Kido, S., Hiraoka, Y., Ogawa, M., Sakai, Y., Yoshimura, Y., Aiso, S., 1998. Cloning and characterization of mouse mSox13 cDNA. Gene 208, 201–206.

Kunisada, T., Miyazaki, M., Mihara, K., Gao, C., Kawai, A., Inoue, H., Namba, M., 1998. A new human chondrosarcoma cell line (OUMS-27) that maintains chondrocytic differentiation. Int. J. Cancer 77, 854–859.

Lefebvre, V., Huang, W., Harley, V.R., Goodfellow, P.N., de Crombrugghe, B., 1997. SOX9 is a potent activator of the chondrocyte-specific enhancer of the pro alpha1(II) collagen gene. Mol. Cell. Biol. 17, 2336–2346.

Lefebvre, V., Li, P., de Crombrugghe, B., 1998. A new long form of Sox5 (L-Sox5), Sox6 and Sox9 are coexpressed in chondrogenesis and cooperatively activate the type II collagen gene. EMBO J. 17, 5718–5733.

Pevny, L.H., Lovell-Badge, R., 1997. Sox genes find their feet. Curr. Opin. Genet. Dev. 7, 338–344.

Schilham, M.W., Oosterwegel, M.A., Moerer, P., Ya, J., de Boer, P.A., van de Wetering, M., Verbeek, S., Lamers, W.H., Kruisbeek, A.M., Cumano, A., Clevers, H., 1996. Defects in cardiac outflow tract formation and pro-B-lymphocyte expansion in mice lacking Sox-4. Nature 380, 711–714.

Siebert, P.D., Chenchik, A., Kellogg, D.E., Lukyanov, K.A., Lukyanov, S.A., 1995. An improved method for walking in uncloned genomic DNA. Nucleic Acids Res. 23, 1087–1088.

Smits, P., Li, P., Mandel, J., Zhang, Z., Deng, J.M., Behringer, R.R., de Croumbrugghe, B., Lefebvre, V., 2001. The transcription factors L-Sox5 and Sox6 are essential for cartilage formation. Dev. Cell 1, 277–290.

Southard-Smith, E.M., Kos, L., Pavan, W.J., 1998. Sox10 mutation disrupts neural crest development in Dom Hirschsprung mouse model. Nat. Genet. 18, 60–64.

van de Wetering, M., Oosterwegel, M., van Norren, K., Clevers, H., 1993. Sox-4, an Sry-like HMG box protein, is a transcriptional activator in lymphocytes. EMBO J. 12, 3847–3854.

Wagner, T., Wirth, J., Meyer, J., Zabel, B., Held, M., Zimmer, J., Pasantes, J., Bricarelli, F.D., Keutel, J., Hustert, E., Wolf, U., Tommerup, N., Schempp, W., Scherer, G., 1994. Autosomal sex reversal and campomelic dysplasia are caused by mutations in and around the SRY-related gene SOX9. Cell 79, 1111–1120.

Werner, M.H., Burley, S.K., 1997. Architectural transcription factors: proteins that remodel DNA. Cell 88, 733–736.

Wolffe, A.P., 1994. Architectural transcription factors. Science 264, 1100–1101.

Wunderle, V.M., Critcher, R., Ashworth, A., Goodfellow, P.N., 1996. Cloning and characterization of SOX5, a new member of the human SOX gene family. Genomics 36, 354–358.

深屈曲動作におけるPCLの重要性

Dominant role of the PCL during deep knee flexion

名倉　武雄　　Andriacchi TP*　松本　秀男　　芦山　芳昭

慶應義塾大学医学部整形外科　*スタンフォード大学生体工学科

Takeo NAGURA, Thomas P. ANDRICACCHI*, Hideo MATSUMOTO, Yoshiaki TOYAMA

Department of Orthopedic Surgery, Keio University
***Division of Biomechanics, Stanford University**

Dynamic knee loads were evaluated in 39 normal healthy knees during walking, stair-ascending, and deep flexion activities. A four camera system and a force plate were used to obtain knee kinematics and kinetics. Internal joint forces were calculated using a statically determinant knee model. During deep flexion beyond 100 degrees, compressive forces were between 3000 and 4000 N. There were 5 to 30 times more forces (300-1800N) on the PCL during deep flexion compared to the ambulatory activities, while the loads on the ACL were less than 100N during the deep flexion activities. The maximum PCL forces were loaded at between 90-150 degrees during deep flexion. The results indicate that the PCL should have a dominant role during the activities that require flexion more than 100 degrees. The large forces on the PCL should be regarded in the design of total knee arthroplasty that is capable for deep flexion.

key words : Deep flexion（深屈曲）
Joint load（関節負荷）
PCL（後十字靭帯）
Knee（膝関節）

はじめに

PCLはさまざまな日常生活動作において，ACLとともに膝の重要な支持機構として機能していると考えられている。Morrison[3]は歩行，階段昇降中のACL/PCL負荷を推定し，これらの歩行動作中はPCLに300-1200Nの負荷があり，その大きさはACLよりも大きいことを示した。またEscamillaら[2]は各種のエスセザイズ中の靭帯負荷を推定し，90度スクワット中はACLに負荷はなく屈曲60度付近でPCLに平均1800Nの負荷がかかることを示した。しかしながら，100度を超える屈曲動作中の靭帯負荷について調べている研究は少ない。また，近年手術手技とデザインの進歩により人工膝関節置換術（以下TKA）後の可動域は100度以上がスタンダードとなりつつあるが，このような深い屈曲角度においてPCLの切除非切除によらず膝にどのようなストレスがかかっているか知ることは，今後日本人に適した人工関節の開発にあたり非常に重要なポイントである。

本研究では100度以上の屈曲を含む深屈曲動作における膝の力学的負荷，特に十字靭帯の負荷を明らかにすることを目的として，健常者の歩行動作および深屈曲動作中の膝関節負荷を解析した。

対象および方法

膝に異常を有さない健常者39人（男20名，女19名：平均年齢28歳，平均身長1.7m，平均体重658N）を対象とした。20名が歩行動作，19名が深屈曲動作を行った。

動作解析装置（4カメラ＋床反力計）をもちいて膝関節の関節外力および外モーメントを算出した[1,4]。マーカーは6つの表面マーカーを使用した。歩行グループは10Mの平地歩行および25.5cm高のプラットフォームへの昇段を，深屈曲グループは4種類の動作を行った(Fig. 1)。

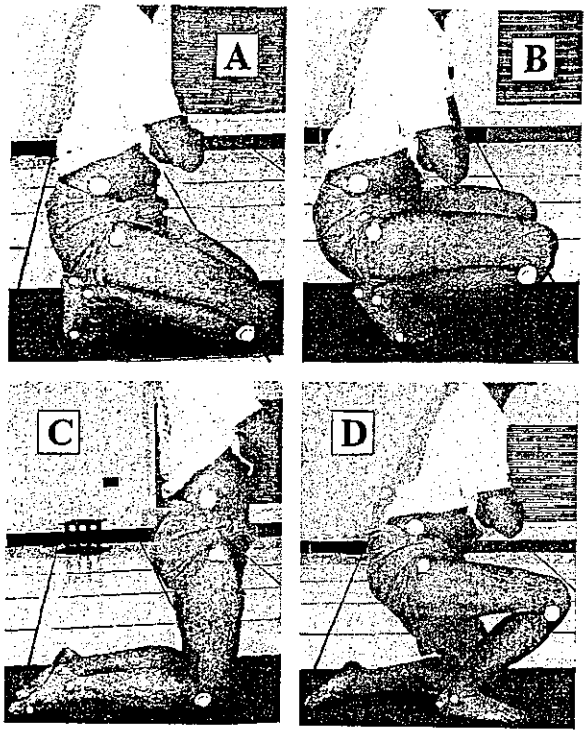

Fig. 1 深屈曲動作

正座位置（A）および正座から立位，または立位から正座への移動（B）。立膝位置（C）および立膝から立位，または立位から立膝への移動（D）。

深屈曲動作として正座位置からの両足での起立（正座起立），また正座への座り（起立正座），立膝位置からの片足での起立（立膝起立）および立膝位置への片足での座り（起立立膝）の4種類を設定した。膝は前2者で約150度まで，後2者では約120度まで屈曲される。

関節内力の推定には，既存の膝モデル[5]を改良したものを用いた。本モデルでは関節外力，外モーメントおよび屈曲角度をインプットとして使用する。膝の伸筋・屈筋力は，膝関節外モーメントに釣り合うものとして計算した。各平面における力およびモーメントの釣り合いから関節内力，ACL・PCL負荷を算出した。統計学的検討には一元配置分散分析を用いた。

結　　果

4種類の深屈曲動作中は膝に平均3000－4000N（体重の4.6－6倍）のCompression forceがかかっていた（Fig. 2）。歩行，階段上昇中のACL負荷はそれぞれ平均108N，159Nであったが，4種類の深屈曲動作中はいずれも100N以下であり，約3分の1の症例では0Nであった（Fig. 3A）。一方PCLの負荷は歩行動作では平均100N前後であったのに対し，深屈曲動作では有意に大きな負荷を示し，特に正座起立と起立正座では歩行・階段上昇の5－30倍となっていた（Fig. 3B）。

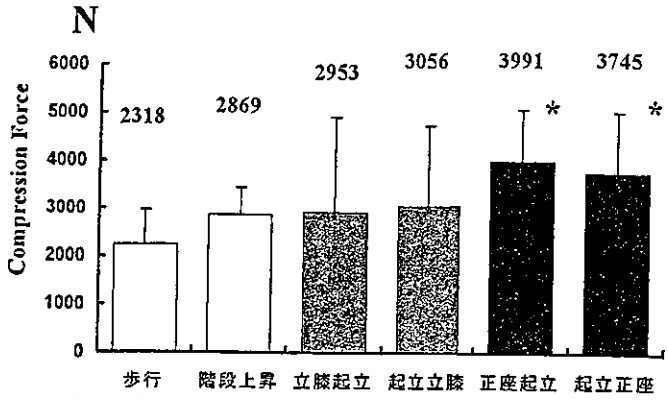

Fig. 2 各動作中の膝関節における Compression force（圧縮力）の比較（単位：ニュートン）

＊歩行・階段上昇に比べ有意差あり（$p<0.05$）

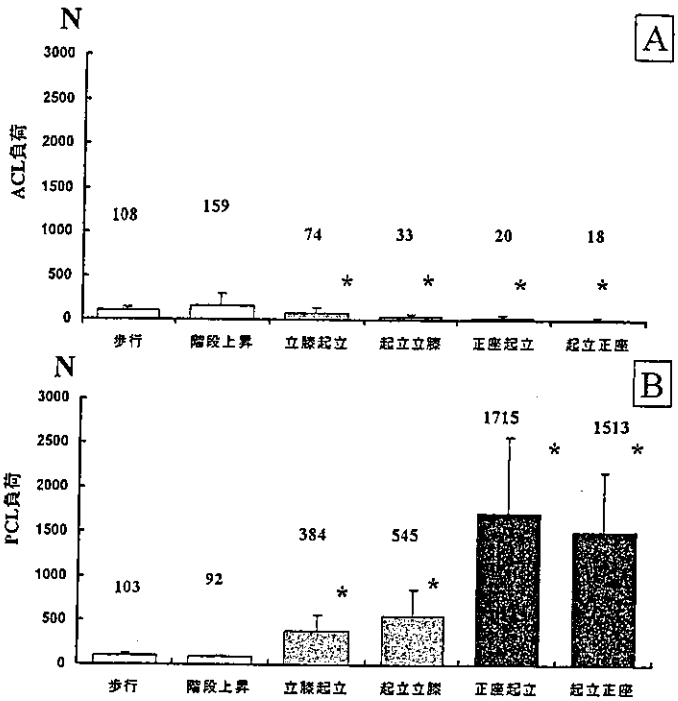

Fig. 3 各動作中のALC負荷（A）およびPCL負荷（B）の比較（単位：　ニュートン）

＊歩行・階段上昇に比べ有意差あり（$p<0.05$）

また ACL・PCL の負荷が最大となる角度は，ACL では歩行，深屈曲動作とも10－40度の間であったが，PCL では立膝動作で90度前後，正座動作では150度前後で最大となっていた（Table 1）。

考　　察

以上の結果より，深屈曲動作中は ACL に比

Table 1 最大靭帯負荷における膝角度 (°)

	ACL	PCL
歩行	18	10
階段上昇	37	43
立膝起立	21	87＊
正座起立	18	147＊

＊歩行，階段上昇に比し有意差あり ($p<0.001$)

Table 2 各動作中の PCL/ACL 負荷比

	PCL / ACL 負荷比	
歩行	0.9	
階段上昇	0.6	
立膝起立	5.2	＊
起立立膝	16.7	＊
正座起立	86.9	＊
起立正座	81.9	＊

＊歩行，階段上昇に比し有意差あり ($p<0.001$)

べ PCL により大きな負荷がかかっていることが明らかになった。各 ADL 動作における PCL・ACL 負荷の比をとると，歩行動作と深屈曲動作の差がより顕著となる (Table 2)。すなわち歩行動作では ACL・PCL はほぼ同等に負荷されていたが，100 度を超える深屈曲動作では PCL の負荷が ACL の 5－100 倍であった。特に 150 度に近い屈曲を行う正座動作では，PCL に極めて大きな負荷がかかり，PCL が膝の安定制御に大きく関与していることが示唆される。

TKA における PCL の切除，非切除が臨床成績に及ぼす影響が議論されている[6]。正常膝をもとにした本研究結果より，TKA においても 100 度を越える屈曲が得られる場合，PCL あるいはそれに相当する部分にかなり大きなストレスが負荷されることが予想される。今後日本人あるいはアジアの生活様式に適した TKA の開発にあたり，考慮すべき点であると考えられた。

今回の検討では膝伸筋・屈筋の筋力が膝外モーメントに釣り合うものとして関節内力を計算しているが，このアプローチでは動作中の拮抗筋活動の影響が評価されない。今後筋電図を動作計測と同時に取得し，拮抗筋を含めた下肢筋の活動を考慮した解析を行う必要があると考えられる。

ま と め

1) 正常膝について歩行動作および 100 度以上の深屈曲動作中の関節内力，靭帯負荷について評価した。

2) 歩行動作中は ACL・PCL に 100N 前後の負荷がみられたが，深屈曲中は PCL に ACL の 5－100 倍の負荷がかかっていた。

3) 100 度以上の深屈曲動作における PCL の重要性が示された。

文　献

1) Andriacchi T.P., Galante J.O., et al.: The influence of total knee-relpacement design on walking and stair-climbing. J Bone Joint Surg Am, 64: 1328-1335, 1982.

2) Escamilla R.F., Fleisig G.S., et al.: Biomechanics of the knee during close kinetic chain and open kinetic chain exercises. Med Sci Sports Exerc, 30: 556-569, 1998.

3) Morrison J.B.: The mechanics of the knee joint in relating to normal walking. J Biomech, 3: 51-61, 1970.

4) Nagura T, Andriacchi T.P., et al.: Mechanical loads at the knee joint during deep flexion. J Orthop Res, 20: 881-886, 2002.

5) Schipplein O.D., Andriacchi T.P.: Interaction between active and passive knee stabilizers during level walking. J Orthop Res, 9: 113-119, 1991.

6) Stiehl B.J., Komistek R.D., et al.: The cruciate ligaments in total knee arthroplasty: a kinematic analysis of 2 total knee arthroplasties. J Arthroplasty, 15: 545-550, 2000.

ELSEVIER

Journal of Orthopaedic Research 20 (2002) 353–356

Journal of Orthopaedic Research

www.elsevier.com/locate/orthres

Effects of different exposures of hyperbaric oxygen on ligament healing in rats

Yoshimasa Ishii [a,*], Takashi Ushida [b], Tetsuya Tateishi [b], Hitoshi Shimojo [c], Yutaka Miyanaga [c]

[a] *Tissue Engineering Research Center, National Institute of Advanced Industrial Science and Technology, Higashi 1-1-1, Tsukuba, Ibaraki 305-8562, Japan*

[b] *Biomedical Engineering Laboratory, Graduate School of Engineering, University of Tokyo, Tokyo, Japan*

[c] *Division of Sports Medicine, Institute of Health and Sport Sciences, University of Tsukuba, Japan*

Accepted 21 June 2001

Abstract

Hyperbaric oxygen (HBO) is a method of augmenting, intermittently, oxygen availability to tissues. We examined the effect of three different HBO exposures on the healing of experimentally induced ligament lacerations in the right hind limb of 44 male Wistar rats. Animals were divided into four groups after ligament injury: (a) control group, animals breathed room air at 1 ATA (atmosphere absolute) in a hyperbaric chamber for 60 min; (b) HBO treatment at 1.5 ATA for 30 min once a day, (c) HBO treatment at 2 ATA for 30 min once a day, (d) 2 ATA for 60 min once a day. At 14 days post-ligament injury, we compared the ligaments of the four treatment groups for gross appearance, histology and expression of pro-α(I) mRNA by northern hybridization. Our results indicate that HBO was effective in promoting ligament healing compared to control ($p < 0.01$). Of these three exposures, HBO at 2 ATA for 60 min was the most effective, resulting in enhanced extra-cellular matrix deposition as measured by collagen synthesis.

Introduction

Hyperbaric oxygen (HBO) therapy has been proposed as a method to promote wound healing [13,23]. Currently, a number of elite athletes are using HBO in an attempt to speed recovery from sprains and contusions, especially with regard to muscle and ligament rupture [3,4,8,10].

Collagen synthesis and fibroblast proliferation are closely related to oxygen availability and cannot proceed without the presence of oxygen [9,16,19]. Oxygen is required for the hydroxylation of proline and lysine, a step that is essential for the synthesis of collagen by fibroblasts [21]. In ischemic wounds, the PO_2 level is lower than in normal tissue due to disrupted circulation and edema. A wound with an oxygen tension 5–20 mm Hg below the normal range 40–45 mm Hg is hypoxic [12]. In vitro, 80 mm Hg was the maximum level of PO_2 considered to be optimal for collagen synthesis and fibroblast growth, being approximately twice the level is found in normal tissue [17]. Kivisaari et al. [14,15] measured tissue gas tensions in vivo by means of a silastic tonometer implanted under the skin of rats to measure gas pressure. Subcutaneous tissue PO_2 levels were increased to 600 mm Hg with exposure to HBO at 2 ATA. In addition oxygen has been shown to be a signal device for cell activation and oxidative phosphorylation [1,2].

In the present study, we examined the effect of HBO at 2 ATA and 1.5 ATA for 60 and 30 min period on the healing of ligament by examining histology and pro-α1 (I) mRNA expression.

Materials and methods

Approval for animal work was obtained from the ethical committee of University of Tsukuba. Forty-four male Wistar rats (aged 8 weeks and weight was 250–270 g) were used in this study. Prior to the experiment, the rats were housed in cages for one week. The animals were anesthetized with pentobarbital intraperitoneally (60 mg/kg) and a longitudinal incision was made over the lateral aspect of the right knee. The patellar ligament was exposed and a laceration (2 mm) was made with a razor-thin knife, transversely in the middle of the patellar ligament, leaving fibers on both sides of the laceration intact. The

* Corresponding author. Tel.: +81-298-612564; fax: +81-298-612565.

E-mail address: yoshi.ishii@aist.go.jp (Y. Ishii).

0736-0266/02/$ - see front matter
PII: S0736-0266(01)00094-8

laceration represents approximately 80% of the ligament's width. The skin was sutured with 4-0 nylon. After recovering from anesthesia, the animals were returned to their cages. The rats were divided into the following groups ($n = 11$ per group):

(Group A) Normobaric room air (control group).
(Group B) Treated with HBO at 1.5 ATA 30 min daily.
(Group C) Treated with HBO at 2 ATA 30 min daily.
(Group D) Treated with HBO at 2 ATA 60 min daily.

In each of the three HBO groups, the total number of applications was 10 over a period of 2 weeks. Rats were fed a standard diet and housed in individual cages.

For HBO treatments, the animals were placed in a cylindrical pressure chamber (P-5100 S; Hanyuda Iron Works, Japan) with a volume of 15.2 l and a continuous oxygen flow of 2 l/min. Three or four animals at a time were put into the chamber and exposed to 100% oxygen daily at a temperature of 25–26°C. The exposures to HBO were as described above. Control animals were put into the chamber without exposure to HBO for 60 min. After HBO treatment, the animals were returned to their cages.

For histological studies, tissues were immersed in 10% formaldehyde and embedded in paraffin, sectioned and dyed with Azan stain. Staining was carried out according to the manufacture's instructions (Muto Pure Chemicals, Japan). After de-paraffination, sections were immersed in a mixture of 10% chromic acid and 10% trichloro-acetic acid for 10 min and washed with dH_2O. Thereafter staining was carried out using Mallory's azocarmin G solution for 60 min and washed by dH_2O, and rinsed with aniline mixed with ethanol and finally with acetic acid also mixed with ethanol. After further washing with dH_2O, samples were immersed in 5% phospho-tungstic acid for at least 60 min and washed with dH_2O. Subsequently samples were stained with Mallory's aniline blue orange G solution for 60 min and then washed again with dH_2O. Samples were then dried in various percentages of ethanol solution. Five animals were used in each group for this experiment.

The repair sites of the four groups were assessed 14 days post-surgery with the remaining six animals in each group. Tissues used for total RNA extraction were carefully divided from the epitenon and taken from the mid-third portion of the patellar ligament transversely. Samples were immediately immersed in liquid nitrogen and subsequently stored at −80°C. Total RNA was extracted using an RNA solution reagent (ISOGEN; Nippon Gene, Japan) according to the manufacturer's instructions. Etachinmate (Nippon Gene, Japan) was used to facilitate total RNA collection. The amount of RNA recovered was determined spectrophotometrically at 260 nm.

For northern hybridization, 1 μg of total RNA was denatured in a solution containing formaldehyde, MOPS, and formamide by heating the mixture to 65°C for 10 min, followed by chilling on ice. RNA samples were electrophoresed in 1.2% (w/v) agarose gel for 3 h at 100 V and transferred to a Hybond N+ membrane (Amersham, Little Chalfont, UK) and subsequently immobilized by UV irradiation. Filters were hybridized at 55°C using Digoxigenin (DIG)- labeled c-DNA probes. Rat pro-α1 (I) positions (530–853 AA), corresponding to the published nucleotide sequence of rat *pα1R1* [6], were obtained by RT-PCR. Probes were labeled using a DIG RNA Labeling Kit (Boehringer Mannheim GmbH Biochemica, Mannheim, FRG) according to the manufacturer's instructions. After washing, the filters were exposed for 3–12 h to Kodak X-OMAT film (Eastman Kodak Rochester, NY, USA).

The amount of pro-α1 (I) mRNA detected by northern hybridization was quantified by densitometry. We measured relative steady-state levels of pro-α1 (I) mRNA extracted from rat patellar ligaments. The mean value of the concentration in control animals was given as a relative unit value of 1 and results are calculated from a comparison with the mean value of the control group. Statistical analysis of the data from the HBO and control groups was performed using ANOVA. Results are expressed as the mean ± standard error of the mean ($n = 6$).

Results

From the gross appearance, the gap portion of the patellar ligaments was filled with scar tissue 2 weeks after wounding in all three of the HBO-treated groups, but this could not be seen in the control group (Fig. 1).

Paraffin sections stained with Azan dye at 14 days post-laceration are shown in Fig. 2. The junction of the wound site and normal ligament were assessed by longitudinal sectioning. It was seen that the laceration began to be filled with collagen fibers and fibroblasts 2 weeks after wounding in all three of the HBO-treated groups, but this was not seen in the control group. At 2 ATA 60 min, the wound was filled with collagen fibers and the ligament appeared to be healing more quickly than with the other two HBO exposures.

The relative expression levels of pro-α1 (I) mRNA are shown in Fig. 3. Although the levels were significantly higher ($p < 0.01$) in the HBO groups than the control group (in order of increasing expression: 1.5 ATA 30 min, 2 ATA 30 min, 2 ATA 60 min) there was no significant difference among the HBO groups themselves.

Discussion

HBO can dissolve oxygen in serum in proportionally to its partial pressure according to Henry's law, firstly enhancing oxygen transport in hypoxic tissue and second, increasing oxygen diffusion through tissue fluids. Clinical applications of HBO include the treatment of chronic refractory osteomyelitis [5,7] compartment

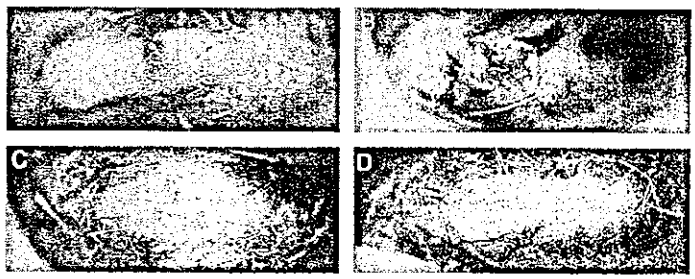

Fig. 1. Gross appearance: (A) Control; (B) 1.5 ATA 30 min; (C) 2 ATA 30 min; (D) 2 ATA 60 min. The wound was created in the middle of the ligament transversely. Left site: femoral site, right site: tibial site.

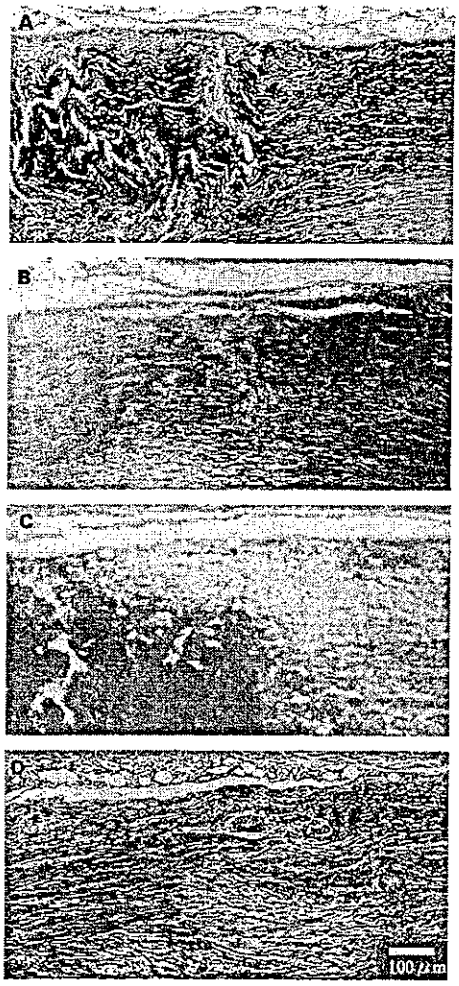

Fig. 2. Histology: (A) Control; (B) 1.5 ATA 30 min; (C) 2 ATA 30 min; (D) 2 ATA 60 min. Left site: normal ligament, right site: healing ligament (×100).

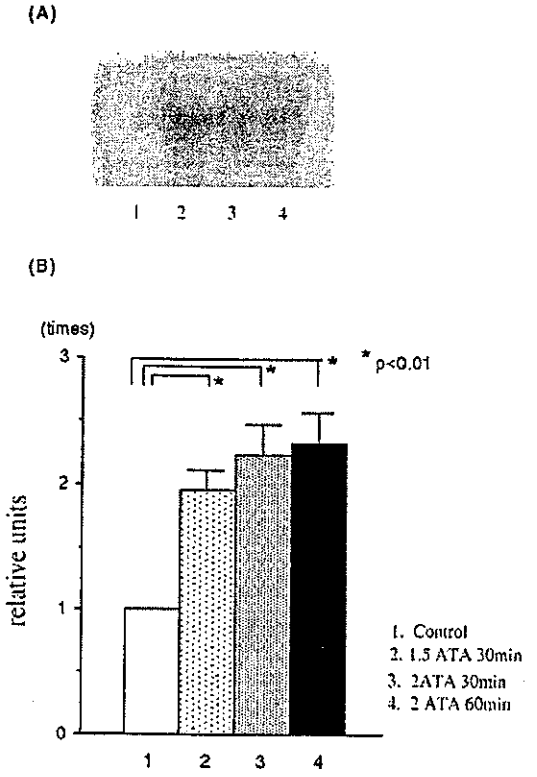

Fig. 3. Northern hybridization: (A) Northern analysis of pro-α1 (I) mRNA levels 14 days post-laceration under the different conditions (DIG label); (B) Expression levels in relative units calculated from the mean value of the concentration of pro-α1 (I) mRNA for the control group. The data represent the mean ±S.E.; $* p < 0.01$ (vs. control).

syndromes [20,24], and as an adjunct for healing of problem wounds [18,22]. Staple and Clement [23] recommended the use of HBO following musculoskeletal injuries in conjunction with physiotherapy and exercise. They recommend 1.5–2 h treatments in the first weeks after injury until healing is complete.

We have previously reported report that HBO accelerated ligament healing histologically, and at 7 and 14 days at the molecular level (pro-α1 (I) mRNA expression) with 2 ATA 60 min treatment once a day [11]. Here we report that 2 ATA for 60 min was more effective than other conditions when studying healing 14 days post-injury. However, the administration of a lower pressure and shorter duration of HBO was also effective compared with the control group.

In conclusion, intermittent HBO at 2 ATA for 60 min is the most effective of three protocols used by assessment of collagen synthesis in the healing ligament. Further studies including biomechanical studies of the effect of HBO on ligament strength are needed. Our results suggest that intermittent oxygen exposure plays a significant role in collagen synthesis during wound healing and my be beneficial in production of extracellular matrix during tissue repair.

Acknowledgements

This study was supported by a grant from the Ministry of Education, Science and Culture in Japan (No. 1248003). We would like to thank Mrs. Rei Hirochika (Tissue Engineering Research Center; TERC, Tsukuba, Japan) for technical assistance and Dr. Rao Sethumadhavan (TERC) and Mr. Leonardo Mendoza (TERC) for their valuable assistance. In addition we recognize the contribution of Dr. John Watson (Smith and Nephew Plc, York, UK) for proof reading this paper.

References

[1] Alberts B, Bray D, Lewis J, Raff M, Roberts K, Watson JD. Molecular biology of the cell. 3rd ed. New York: Gardland; 1994.

[2] Babcock GT, Wikström M. Oxygen activation and the conservation of energy in cell respiration. Nature 1992;356:301–9.
[3] Best TM, Loitz-Ramage B, Corr DT, Vanderby R. Hyperbaric oxygen in the treatment of acute muscle stretch injuries. Result in acute an animal model. Am J Sports Med 1998;263:67–372.
[4] Borromeo CN, Ryan JL, Marchetto PA, Peterson R, Bove AA. Hyperbaric oxygen therapy for acute ankle sprains. Am J Sports Med 1997;25:619–25.
[5] Davis JC, Refractory osteomyelitis of the extremities and the axial skeleton. In: Davis JC, Hunt TK, editors. Hyperbaric oxygen therapy. Bethesda: Undersea Medical Society; 1977. p. 217–77.
[6] Genovese C, Rowe D, Kream B. Construction of DNA Sequences complementary to rat α1 and α2 Collagen mRNA and their use in studying the regulation of type I collagen synthesis by 1,25-Dihydroxyvitamin D. Biochemistry 1984;23:6210–6.
[7] Hamblin DL. Hyperbaric oxygen: its effect on experimental staphyrococcal osteomyelitis in rats. J Bone Joint Surg (AM) 1968;50:1129–41.
[8] Horn PC, Webster DA, Amin HM, Mascia MF, Werner FW. Fortino: Effect of hyperbaric oxygen on medial colateral ligament healing in a rat model. Clin Orthop 1999;360:238–42.
[9] Hunt TK, Zederfeldt B, Goldstick TK. Oxygen and healing. Am J Surg 1969;118:521–5.
[10] Ishii Y, Miyanaga Y, Asano K, Shimojo H, Shiraki H. Metabolic effects of hyperbaric oxygen on muscle tear in the hind limb of rats. Adv Exer Sports Physiol 1998;4:11–5.
[11] Ishii Y, Miyanaga Y, Shimojo H, Ushida T, Tateishi T. Effect of hyperbaric oxygen on procollagen messenger RNA levels and collagen synthesis in the healing of rat tendon laceration. Tissue Eng 1999;5:279–86.
[12] Jain KK. Textbook of hyperbaric medicine. 3rd ed. Seattle: KK. Hogrefe & Huber Publishers; 1999.
[13] James PB, Scott B, Allen MW. Hyperbaric oxygen therapy in sports injuries. Physiotherapy 1993;79:571–2.
[14] Kivisaari J, Niiniskoski J. Use of silastic tube and capillary sammpling technique in the measurement of tissue P_{O_2} and P_{CO_2}. Am J Surg 1973;125:623–7.
[15] Kivisaari J, Niinikoski J. Effects of hyperbaric oxygenation and prolonged hypoxia on the healing of open wounds. Acta Chir Scand 1975;141:14–9.
[16] LaVan FB, Myers B. Oxygen and wound healing. Clin Plast Surg 1990;17:463–72.
[17] Mehm WJ, Pimsler M, Becker RL, Lissner CR. Effect of oxygen on in vitro fibroblast cell proliferation and collagen biosynthesis. J Hyper Med 1988;3:227.
[18] Meltzer T, Myers B. The effect of hyperbaric oxygen on bursting strength and rate of vascularization of skin wounds in rat. Am Surg 1988;52:659–61.
[19] Niiniskoski J. Effect of oxygen on wound healing and formation of experimental granuration tissue. Acta Physiol Scand 1969;(Suppl 334):1–72.
[20] Nylander G, Lewis D, Nordström H, Larsson J. Reduction of edema with hyperbaric oxygen. Plast Reconstr Surg 1985;76:596.
[21] Prockop D, Kaplan A, Udenfriend S. Oxygen-18 studies on the convension of proline to hydroxyproline. Biochem Biophys Res Commun 1992;9:162–6.
[22] Quirinia A, Viidik A. The effect of hyperbaric oxygen on different phases of healing of ischaemic flap wounds and incisional wounds in skin. Br J Plast Surg 1995;48:583–9.
[23] Staple J, Clement D. Hyperbaric oxygen chambers and the treatment of sports injuries. Sport Med 1996;22:219–27.
[24] Strauss MB, Hargens AR, Gershuni DH, Greenberg DA, Crenshaw AG, Hart GB, Akeson WH. Reduction of skeletal muscle necrosis using intermittent hyperbaric oxygen in a model compartment syndrome. J Bone Joint Surg (AM) 1983;65:656–62.

JOURNAL OF CELLULAR PHYSIOLOGY 194:45–53 (2002)

Use of Isolated Mature Osteoblasts in Abundance Acts as Desired-Shaped Bone Regeneration in Combination With a Modified Poly-DL-Lactic-Co-Glycolic Acid (PLGA)-Collagen Sponge

KENSUKE OCHI,[1,2] GOUPING CHEN,[3] TAKASHI USHIDA,[4] SATOSHI GOJO,[5] KAORU SEGAWA,[6] HITOSHI TAI,[7] KENJU UENO,[7] HIROYUKI OHKAWA,[8] TAISUKE MORI,[1] AKIRA YAMAGUCHI,[9] YOSHIAKI TOYAMA,[2] JUN-ICHI HATA,[1] AND AKIHIRO UMEZAWA[1]*

[1]*Department of Pathology, Keio University School of Medicine, Tokyo, Japan*
[2]*Department of Orthopaedics, Keio University School of Medicine, Tokyo, Japan*
[3]*Tissue Engineering Research Center, AIST, Amagasaki, Japan*
[4]*Biomedical Engineering Laboratory, Graduate School of Engineering, University of Tokyo, Tokyo, Japan*
[5]*Department of Cardiac Surgery, Saitama Medical Center, Saitama, Japan*
[6]*Department of Microbiology, Keio University School of Medicine, Tokyo, Japan*
[7]*Fuji-Gotemba Research Laboratories, Chugai Pharmaceutical Co., Ltd., Shizuoka, Japan*
[8]*Product Research Lab., Chugai Pharmaceutical Co., Ltd., Tokyo, Japan*
[9]*Division of Oral Pathology and Bone Metabolism, Nagasaki University Graduate School of Biomedical Sciences, Nagasaki, Japan*

Controlled regeneration of bone or cartilage has recently begun to facilitate a host of novel clinical treatments. An osteoblast line, which we isolated is able to form new bone matrix in vivo within 2 days and exhibits a mature osteoblast phenotype both in vitro and in vivo. Using these cells, we show that cuboidal bones can be generated into a predesigned shaped-bone with high-density bone trabeculae when used in combination with a modified poly-DL-lactic-co-glycolic acid (PLGA)-collagen sponge. PLGA coated with collagen gel serves as a good scaffold for osteoblasts. These results indicate that mature osteoblasts, in combination with a scaffold such as PLGA-collagen sponge, show promise for use in a custom-shaped bone regeneration tool for both basic research into osteogenesis and for development of therapeutic applications. J. Cell. Physiol. 194: 45–53, 2002.

The concept of regenerative medicine refers to the cell-mediated restoration of damaged or diseased tissue, and practically, regeneration of bone and cartilage may be one of the most accessible approaches. Candidate cell sources for regeneration of tissue include embryonic stem cells, fetal cells or adult cells such as marrow stromal cells (Bianco and Robey, 2000), each of which has both benefits and drawbacks.

Multipotent mesenchymal stem cells have recently been isolated from adult marrow and were shown to proliferate extensively, and to maintain the ability to differentiate into multiple cell types such as osteoblasts, chondrocytes, and myoblasts in vitro (Umezawa et al., 1992; Pittenger et al., 1999; Bianco and Robey, 2000). We have also shown that stromal cells are able to generate cardiomyocytes and endothelial cells (Makino et al., 1999), neuronal cells (Kohyama et al., 2001), and adipocytes (Umezawa et al., 1991). Clinical trials have already been performed using marrow stromal cells to treat patients with osteogenesis imperfecta (Horwitz et al., 1999) and osteoporosis (Canalis, 2000; Rodan and Martin, 2000). Thus, marrow stromal cells are expected to be a good source of cell therapy in addition to embryonic stem cells and fetal cells (Pittenger et al., 2000).

Humoral factors have also been used to induce bone formation (Yamaguchi et al., 2000). Bone morphogenetic proteins (BMPs) such as BMP-7 and BMP-2 induce osteogenesis in vivo when added them to matrix implants (Service, 2000). Treatment of simple collagen matrices with BMPs prompted rapid healing of bone defects in animal models. In human, implants of a

Contract grant sponsor: Ministry of Education, Culture, Sports, Science, and Technology; Contract grant numbers: 11557021, 13470053, 13022264, 11167274; Contract grant sponsor: Keio University Special Grant-in-Aid for Innovative Collaborative Research Project; Contract grant sponsor: National Grant-in-Aid for the Establishment of a High-Tech Research Center at Private Universities.

*Correspondence to: Akihiro Umezawa, Department of Pathology, Keio University, School of Medicine, 35 Shinanomachi, Shinjuku-ku, Tokyo, 160-8582, Japan.
E-mail: umezawa@1985.jukuin.keio.ac.jp

Received 10 April 2002; Accepted 1 August 2002

DOI: 10.1002/jcp.10185